*J. Plasma Physics* (2007), *vol.* 73, *part* 3, *pp.* 295–306.  
doi:10.1017/S0022377806004569 First published online 17 May 2006 Printed in the United Kingdom

# Tokamak turbulence at the scrape-off layer in TCABR with an ergodic magnetic limiter

M. V. A. P. HELLER, I. L. CALDAS, A. A. FERREIRA, E. A. O. SAETTONE and A. VANNUCCI
Institute of Physics, University of São Paulo, C. P. 66318, 05315-970 São Paulo, SP, Brazil

(Received 10 February 2006, accepted 02 March 2006)

**Abstract.** The influence of an ergodic magnetic limiter (EML) on plasma turbulence is investigated in the *Tokamak Chauffage Alfvén Brésilien* (TCABR), a tokamak with a peculiar natural superposition of the electrostatic and magnetic fluctuation power spectra. Experimental results show that the EML perturbation can reduce both the magnetic oscillation and the electrostatic plasma turbulence. Whenever this occurs, the turbulence-driven particle transport is also reduced. Moreover, a bispectral analysis shows that the nonlinear coupling between low- and high-frequency electrostatic fluctuations increases significantly with the EML application.

## 1. Introduction

It is generally believed that the existence of plasma edge turbulence is critical for tokamak performance and can cause strong particle transport, reducing the magnetic energy of the confined plasma [1–3]. Despite the recent theoretical [4–6] and experimental progress [7] on the understanding of this turbulence, its control has not yet been achieved.

Although in some toroidal devices such as the reversed field pinches (see, for example, the experiments in EXTRAP1 [8]) both electrostatic and magnetic fluctuations directly contribute to the edge transport, in tokamaks this effect is typically determined only by electrostatic fluctuations. However, in some tokamak experiments correlations between electrostatic and magnetic fluctuations at the plasma edge have been reported [9–11]. Whenever these correlations are present, the magnetic fluctuations affect the electrostatic fluctuations. Thus, in the tokamak TEXT, magnetic perturbations created by an ergodic magnetic limiter (EML), with a dominant mode, were observed to modulate the electrostatic plasma edge turbulence [11].

In the former Brazilian tokamak, TBR, a partial superposition of the broadband magnetic and electrostatic power spectra was observed. In this tokamak it was also observed that the correlations and nonlinear coupling between these fluctuations were reduced by the magnetic perturbation created by resonant helical windings [12–14].

Recently, experiments carried out in the CASTOR tokamak showed evidence of long potential structures aligned with the magnetic field and the influence of these structures on the turbulence-induced particle transport was also reported [15].

Considering these remarks, it seems important to continue investigating the application of external magnetic perturbations to control turbulence and transport within the tokamak plasma edge. One promising approach is the application of stochastic magnetic fields at the plasma boundary, by employing specially designed coils, to reduce the inward impurity transport and, possibly, to prevent plasma instabilities. Recently, it was shown that boundary layers, created by these coils, improved the plasma confinement [16–19] and even stabilized the edge localized modes [20]. In particular, EMLs [21, 22] have been used to apply stochastic fields at the tokamak plasma edge, improving plasma confinement in TextUp [1, 23] and HYBTOK-II [24–26]. Experiments in TORE-SUPRA showed that the plasma performance could be improved or degraded by resonant magnetic perturbations created by an ergodic divertor, depending on the plasma configuration [27, 28]. Moreover, the effect of rotating helical magnetic field on the turbulence fractal structure and transport in the tokamak edge plasma has been studied in the tokamak HYBTOK-II [29].

In this work, an EML [22] was recently constructed and employed to control magnetohydrodynamic (MHD) activity and to study disruptions in the TCABR tokamak [30]. The EML installed was projected to create magnetic perturbations with a dominant $m = 3$ poloidal mode at the plasma border. Therefore, it was possible to investigate the influence of the resonant field created by this EML on the plasma scrape-off layer turbulence and also on the particle transport induced by this turbulence.

For this task, a system of probes was used to measure the electrostatic fluctuations and basic plasma parameters, such as density, potential and temperature. The experimental data were treated by using wavelet spectral analysis to quantify the turbulence-driven radial particle flux and also to verify the existence of nonlinear wave–wave couplings, through bispectral analysis. In the following, we characterize a peculiar feature of the electrostatic and magnetic oscillations observed in the TCABR tokamak, namely, the superposition of their power spectra. Finally, we use this special feature and the EML installed in TCABR to investigate the possibility of controlling the plasma turbulence.

In TCABR both natural and externally applied magnetic perturbations can modulate electrostatic turbulence, changing the plasma edge characteristics [31,32]. These perturbations also reduce the plasma edge turbulence, modify its power spectra, and reduce the turbulence-driven transport.

The outline of this paper is as follows: we give a brief description of the experiment and data acquisition in Sec. 2; the power spectra and transport alterations are described and discussed in Secs 3 and 4. In Sec. 5 we summarize the conclusions of this work.

## 2. Experiment

The experiment was performed in an hydrogen circular plasma in TCABR [33] (major radius $R = 0.61$ m, minor radius $a = 0.18$ m). Typically, the plasma current was 90 kA, the current duration 100 ms, the hydrogen filling pressure $3 \times 10^{-4}$ Pa, and the toroidal magnetic field $B_t = 1.1$ T. The probe system was installed in the equatorial region of the tokamak at 90° from the limiter. The multipin Langmuir probe was composed of a triple probe that measures mean density, plasma potential, and electron temperature; while two pins were used to measure the fluctuations of

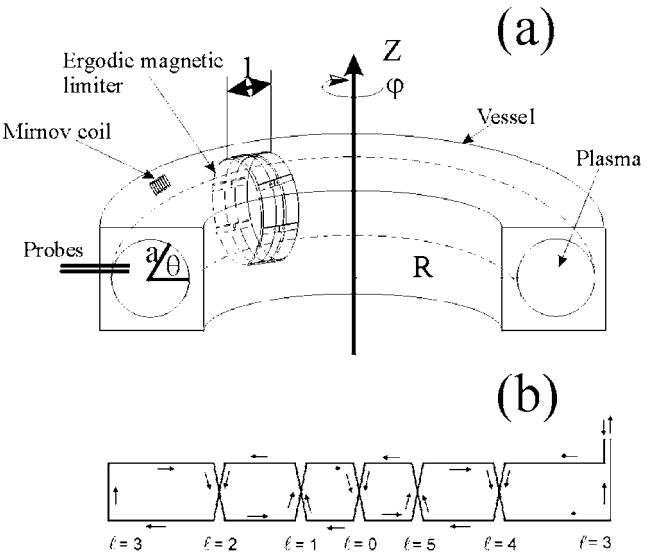


**Figure 1.** (a) A schematic diagram of the experimental set-up, probes, Mirnov coil, and EML. (b) A schematic diagram of the EML geometry of TCABR. The arrows show the current direction and $l$ is the segment number.

the floating potential, with the third one measuring the ion saturation current fluctuations. The probes mounted on a movable shaft could be moved, from shot to shot, in the range $r = 15 \times 10^{-2}$ m to $r = 23 \times 10^{-2}$ m (distance measured in reference to the center of the plasma column) [34]. Figure 1(a) shows the scheme of the experimental set-up (giving emphasis on the positioning of the probes, Mirnov coils, and ergodic magnetic limiter). The magnetic field fluctuations were measured using a set of Mirnov coils located at ≈45° from the probe system position. The experimental data were recorded using ADC (Analogic Digital Converter) modules in 12 bit VME boards, with a maximum sampling rate of 1 MHz. The bandwidth of the fluctuation measuring circuits was approximately 300 kHz, to avoid aliasing. Thus, we typically analyzed 50 000 points in every discharge. We split the data into consecutive segments of 1.02 ms and applied wavelet analysis to each segment.

In this work, we investigated the scrape-off layer turbulence changes introduced by the EML. The EML system was installed inside the TCABR vacuum vessel at approximately 10° from the probe system. This system was projected to create a magnetic perturbation with a dominant $m = 3$ poloidal mode at the plasma edge and, in its construction, the EML current straight segments were distributed along the poloidal direction, at one toroidal position, taking into account the effects produced by the tokamak toroidal geometry [30, 35]. The corresponding power supply was built using 220 electrolytic capacitors (2.85 mF, 450 V) and five 2.5 mH inductors. Therefore, a current of 3 kA maximum could be generated for about 50 ms. A schematic drawing of the EML geometry is shown in Fig. 1(b) (the arrows indicate the current direction and $l$ is the segment number). A more complete description of the EML system is given in [35].

The figures presented in this work correspond to data fluctuations measured within the scrape-off layer, at $r/a = 1.05$. The mean values of density, temperature, and plasma potential are, respectively, $n_e \approx 8.5 \times 10^{17}$ m$^{-3}$, $T_e \approx 18$ eV, and

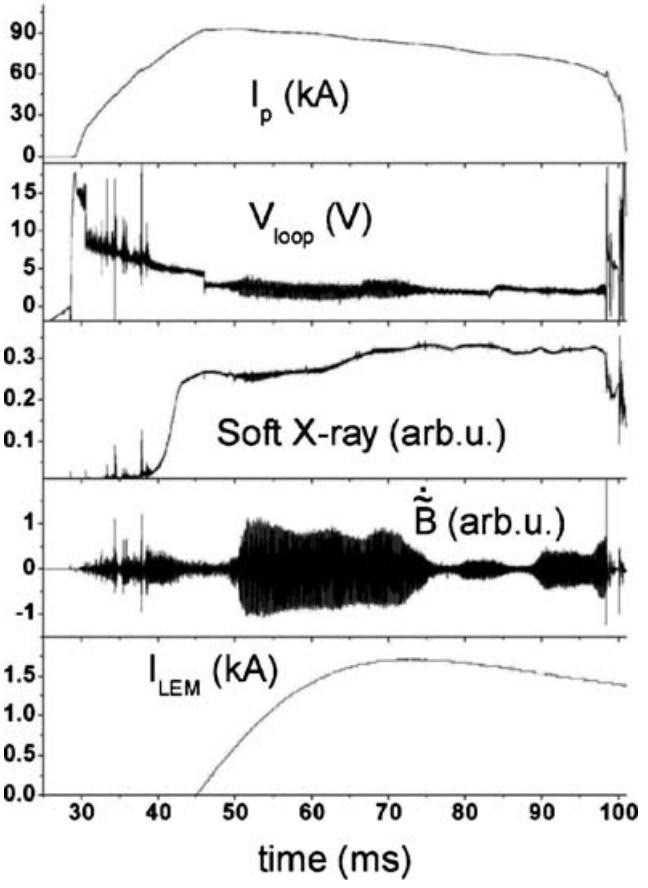


**Figure 2.** Plasma temporal parameters, plasma current $I_\mathrm{p}$, $V_\mathrm{loop}$, soft X-rays, $dB/dt$, and the current in the EML, for an analyzed discharge.

$V_\mathrm{p} \approx 60$ V. Some characteristic plasma signals of the analyzed discharges ($V_\mathrm{loop}$, soft X-rays, $dB/dt$, plasma current $I_\mathrm{p}$, and EML current) are shown in Fig. 2. Whenever it is interesting to compare different turbulent behavior, data from other radial positions are also considered.

## 3. Effect of the EML on the scrape-off layer turbulence

With the application of the EML, we observe attenuation of the Mirnov oscillations and significant changes in the electrostatic turbulence. The time-averaged plasma density, $n_\mathrm{e}$, increases moderately (by less than 15%) while the poloidal electrical field, $E_\theta$, and the electron temperature, $T_\mathrm{e}$, are not much affected. To describe the fluctuation changes in the TCABR tokamak, we use spectral and statistical analyses of the electrostatic turbulence and Mirnov oscillations.

As shown in [31], an interesting peculiarity exhibited by our experimental data is the electrostatic turbulence modulation by the magnetic field fluctuations. The magnetic fluctuations, measured by Mirnov coils, have $m = 3$ and $m = 4$ dominant poloidal modes.

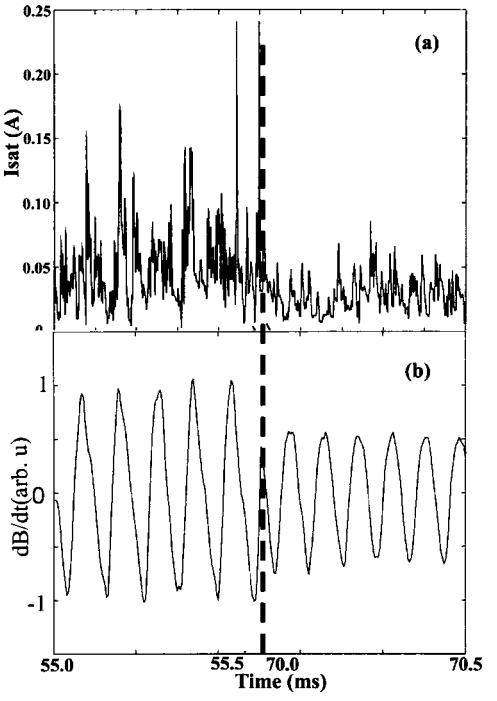


**Figure 3.** (a) Ion saturation current and (b) Mirnov fluctuations for two time intervals without and with (after the dashed line) the EML perturbation.

The influence of the EML perturbation on the electrostatic and magnetic fluctuations can be seen in Fig. 3. This figure shows a sample part of the ion saturation current and the Mirnov fluctuations prior to and after the EML starts acting upon the plasma confinement, as indicated by the dashed lines. Note also that formerly the electrostatic signals exhibit a high frequency together with a burst sequence. Interestingly, the EML perturbation reduces both the electrostatic and Mirnov fluctuation amplitudes.

As usual, the Probability Distribution Functions for the fluctuations are not symmetric. By applying the EML, the skewness for the fluctuating ion saturation current increased from $S = 2.7$ to $S = 3.6$. For the floating potential, the value of $S = 1.6$ remains the same.

In this work, the turbulence analysis is based on correlation techniques applied to both floating potential and ion saturation current fluctuations. We obtain the time behavior of the fluctuations by splitting the data into segments of 1024 data points ($\approx$1.02 ms) and applying wavelet analysis to each segment [36]. The use of wavelet analysis has been verified to be very convenient in investigating any possible spectral alteration during a single discharge.

Figure 4 shows, comparatively, the obtained electrostatic and magnetic fluctuation spectra. While the magnetic fluctuation spectrum is concentrated around 10 kHz (Mirnov frequency – solid curve), the electrostatic fluctuations exhibit a broadband spectrum (dashed curve), part of it related to the Mirnov oscillation frequency. This observation confirms that, in TCABR, electrostatic fluctuations are modulated by the magnetic fluctuations.

Figure 5 shows the potential fluctuation spectra for plasma discharges without (from 50.0 to 51.2 ms) and with (from 70.0 to 71.2 ms) the EML application, related

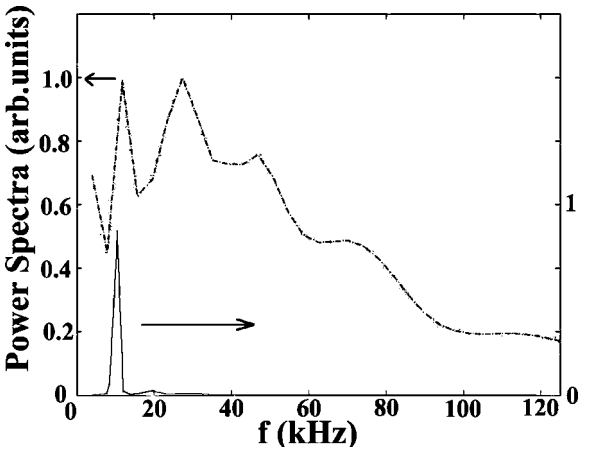


**Figure 4.** Superposition of the power spectra of Mirnov ( —— ) and potential fluctuations ( - - - ) at $r/a = 1.05$.

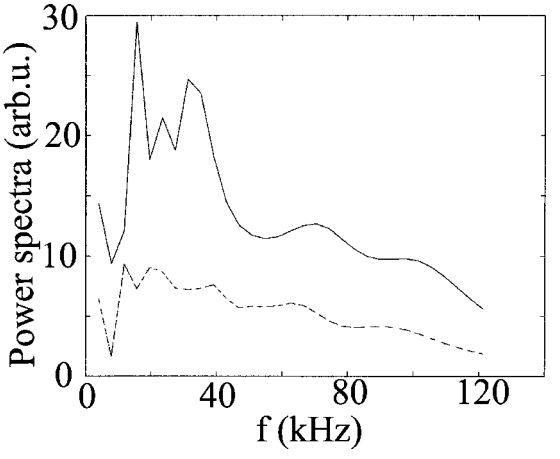


**Figure 5.** Superposition of the power spectra of potential fluctuations for two chosen intervals of 1.02 ms, one without ( —— ) and the other with ( - - - ) the EML perturbation.

to experimental data measured at the radial position $r/a = 1.05$. These spectra indicate a considerable reduction of the electrostatic fluctuations when the EML is applied. These results presented in Figs 4 and 5 highlight the importance of the turbulence component with the magnetic fluctuation frequency in comparison with other frequency ranges. This spectrum characteristic is an indication of a coupling between the magnetic and the turbulent fluctuations, as considered in [4, 5].

Furthermore, by using the two-point technique, we use the wavenumber frequency spectrum to calculate the average value of the poloidal phase velocity of the turbulence, $v_{\mathrm{ph}} = w/k$. Figure 6 shows the evolution of this velocity before and after the EML perturbation is introduced. This observed velocity reduction is mainly due to the alteration in the poloidal wavenumber spectrum with the increase of the average value $k$. There is evidence that the poloidal wavenumber spectra and the corresponding phase velocities depend on the magnetic rational

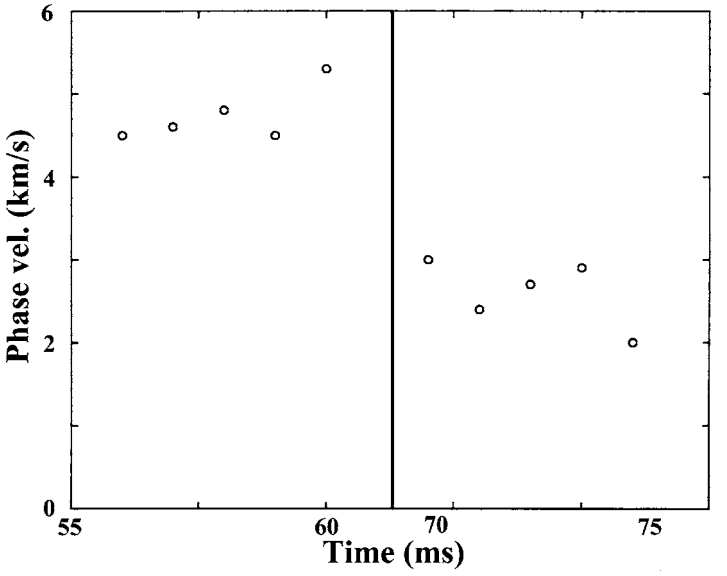


**Figure 6.** Time evolution of the poloidal phase velocity without and with (after the solid line) EML. Statistical errors are estimated to be smaller than 15%.

surface positions [37]. Thus, in our case, the observed alteration in phase velocity may be due to the magnetic topology modification introduced by the EML.

The coherence between the fluctuating ion saturation current and the floating potential is approximately 0.6 for low frequencies up to 50 kHZ and much lower for higher frequencies. This coherence for low-frequency turbulence is reduced by the EML. Thus, the turbulence-driven transport is concentrated in this frequency range.

Finally, to detect evidence of phase coupling between wavelet components of different scale lengths, possibly present in the electrostatic turbulence, we calculated the bispectra and bicoherences between two frequencies and their sum or difference [34,38]. Figure 7 shows the superposition of the summed autobicoherence, of the potential fluctuations, before (dashed curve) and after (solid curve) the EML application. Alterations in high-frequency modes are mainly responsible for the nonlinear coupling increase when the EML perturbations are applied. The bicoherence changes are negligible for low frequencies around the Mirnov frequency. This is confirmed by comparing the nonlinear coupling calculations using (or not) filtered data, excluding (or not) frequencies within the Mirnov frequency range. The nonlinear behavior increase and the phase velocity reduction, observed in our experiment, is expected for drift-wave multimode spectra in two-dimensional turbulence [39].

Comparisons of the experimental bicoherence change, caused by the stochastic magnetic perturbations created by the EML perturbation, and predictions of different turbulence and transport models may provide an indication of whether these models are suitable for describing the influence of stochastic magnetic fields on the electrostatic turbulence [3,40]. Moreover, the bicoherence values could be related to the parameters, such as the coupling strength, of a given turbulence model [41,42]. Finally, the bicoherence evolution has also been considered to identify alterations

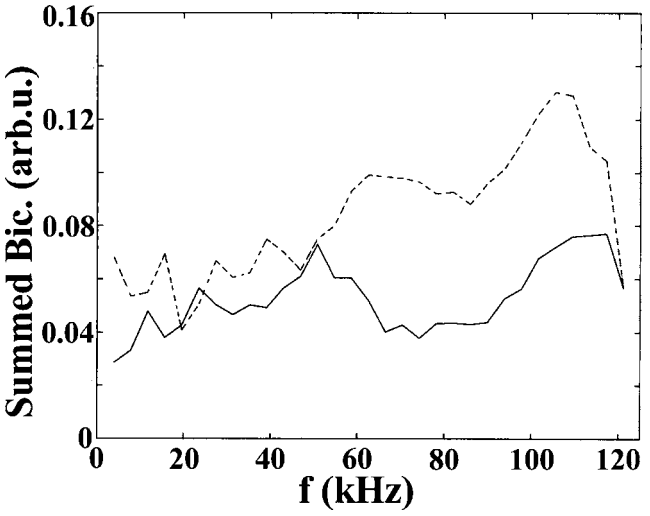


**Figure 7.** Superposition of the summed autobicoherence for potential fluctuations without ( —— ) and with ( - - - ) EML.

in the propagation of spatial structures with dynamic quadratic wave interactions [40].

## 4. Particle transport

To verify the EML influence on the particle flux at the scrape-off layer, during a discharge, we calculate the transport power spectrum. We estimate this transport from the turbulent electrostatic fluctuations analyzed in this work. The radial particle flux,

$$\Gamma = \langle \tilde{n} v_r \rangle, \tag{4.1}$$

driven by the density and plasma potential fluctuations, $\tilde{n}$ and $\varphi$, is obtained by calculating the fluctuating radial drift velocity

$$v_r = E_\theta / B_t \quad (E_\theta = k\varphi). \tag{4.2}$$

In this section we use spectral analysis to calculate $\Gamma$ from the equations

$$T_r(f) = 2k|S_{n\varphi}| \sin(\theta_{n\varphi})/B_\mathrm{t} \tag{4.3}$$

$$\Gamma = \int_0^\infty T_r(f)\, df \tag{4.4}$$

where $k$ is the plasma potential poloidal wavenumber, $S_{n\varphi}$ and $\theta_{n\varphi}$ are the wavelet cross spectrum and phase angle between the density and potential fluctuations, and $B_\mathrm{t}$ is the toroidal magnetic field.

Figure 8 shows the superposition of the transport spectra obtained for two time intervals of 1.02 ms each, prior to and after the EML application. This perturbation reduces the transport by ≈70%. The observed transport reduction due to the EML perturbation occurs mainly in the low-frequency range up to 50 kHz (which comprises the Mirnov frequency around 10 kHz). For the analyzed discharges, this reduction of transport, which is observed after the EML application, is mainly

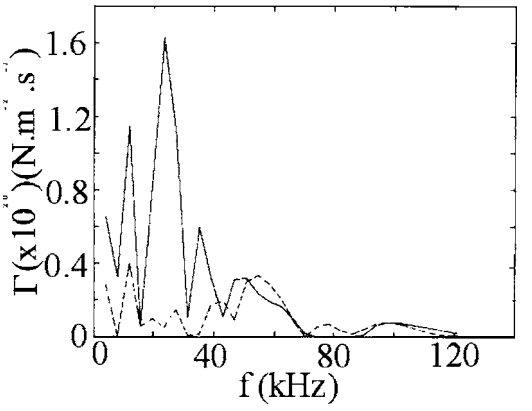


**Figure 8.** Superposition of particle transport spectra for two time intervals of 1.02 ms, one without ( —— ) and the other with ( - - - ) EML.

a consequence of the change of the phase angle, $\theta_{n\varphi}$, between the density and potential fluctuations, with angle inversion for low-frequency ranges. Thus, in the analyzed experiment, the influence of Mirnov fluctuations on the turbulence, and consequently on its driven transport, is evident. Although this effect was observed for several discharges, it was only measured at a fixed poloidal position in the scrape-off layer. Eventually, the total transport reduction may be less significant due to its variation with the poloidal position. This consideration seems to be confirmed by the observed increase of only 15% for the above-mentioned average chord density. In conclusion, the slight global change indicated a local nature of the measured turbulent transport, as observed, for example, in the stellarator TJ-II [37].

Part of the particle transport presented in Fig. 8 may be convective, associated with plasma structures whose propagation is responsible for the intermittent bursts commonly observed in the electrostatic fluctuation signals registered by the Langmuir probes [43–46]. This convective transport can be estimated from the radial displacement of the plasma structures associated with the bursts.

Here we also analyze the bursts in the scrape-off layer fluctuation signals and calculate the transport associated with them. Then, we compare this transport during a plasma discharge prior to and after the EML application. Thus, we estimate the part of the total turbulence-driven transport that can be associated with the bursts. However, to do so it is first necessary to identify the bursts and their statistics [36, 43–46]. To discriminate the bursts, we select the fluctuating density with amplitudes equal to, or greater than, 3.0 times the fluctuation standard deviation. Thus, we use (4.1) and (4.2) to obtain, directly from the measured data, the radial velocities of the bursts and the corresponding particle transport.

Without the external perturbation, the ratio $R_\Gamma$ of the convective transport, in respect to the overall transport, is $\approx$16% near the plasma edge. When the EML perturbation is applied, the contribution of bursts to the total transport does not vary significantly in the scrape-off layer. Finally, it is worth saying that in most shots, prior to or after the perturbation, the bursts observed in the experimental data comprise about 5% of the time series.

The Mirnov oscillations are mainly composed of resonant low poloidal wavenumbers that create magnetic islands inside the plasma and a stochastic layer at the

plasma edge. The island size and the extension of the stochastic layer are reduced with the resonant mode amplitude. Thus, this stochastic layer reduction, observed when the EML is applied, reduces the escape of magnetic field lines to the plasma wall and, consequently, diminishes the associated particle transport [27, 28, 47].

## 5. Conclusions

In the TCABR tokamak, the Mirnov fluctuation frequency range is restricted to a small range in contrast to the electrostatic turbulence frequency broadband spectrum. On the other hand, the EML installed in TCABR is used to reduce the magnetic fluctuations. Combining these two features, we show that it is also possible to control electrostatic turbulence at the TCABR scrape-off layer.

We have analyzed the spectral characteristics of the scrape-off layer electrostatic turbulence in TCABR. The magnetic perturbation is observed to change the electrostatic fluctuation power spectra, reducing turbulence amplitudes and phase velocities. We have observed that the electrostatic turbulence is modulated, in the frequency range around 10 kHz, by the Mirnov oscillations, whose power spectra appear in the same range. Bispectral analysis of the plasma edge electrostatic fluctuations show the occurrence of nonlinear coupling between low- and high-frequency electrostatic fluctuations. This coupling even increases with the EML application. This effect suggests that other nonlinear effects, such as the coupling between the magnetic and the turbulence fluctuations, may be present under our experiment conditions. However, turbulence alterations due to modification in the plasma current gradient on the rational surfaces that influences the tearing mode stability cannot be discarded.

The modulation of electrostatic turbulence by the magnetic oscillations reduces the particle transport. The relative contribution of the radial transport associated with the intermittent bursts is not much affected by the EML fields. The observed electrostatic turbulence and transport spectra reductions may be explained as due to alterations in the magnetic configuration at the plasma edge caused by the EML. Recently, other evidence of the influence of the magnetic configuration on the plasma edge turbulence have been observed by modifying the position of the stochastic boundary layer in the tokamaks TEXTOR [16] and DIIID [20] or the magnetic separatrix in the tokamak CASTOR [20].

*Acknowledgements*

The authors are indebted to the TCABR team for the use of laboratory facilities. This work was partially supported by the Brazilian governmental agencies FAPESP (Fundação de Amparo à Pesquisa do Estado de São Paulo) and CNPq (Conselho Nacional de Pesquisa).

## References

[1] Wootton, A. J., Mc Cool, S. C. and Zheng, S. 1991 *Fusion Technol.* **19**, 473.
[2] Wagner, F. and Stroh, U. 1993 *Plasma Phys. Control. Fusion* **35**, 1321.
[3] Horton, W. 1990 *Phys. Rep.* **192**, 1.
[4] Camargo, S. J., Scott, B. D. and Biskamp, D. 1996 *Phys. Plasmas* **3**, 3912.
[5] Camargo, S. J., Biskamp, D. and Scott, B. D. 1995 *Phys. Plasmas* **2**, 48.

[6] Sarazin, Y. et al. 2003 *J. Nucl. Mater.* **313–316**, 796.

[7] Beyer, P., Garbet, X., Benkadda, S., Ghendrih, P. and Sarazin, Y. 2002 *Plasma Phys. Control. Fusion* **44**, 2167.
Bourdelle, C. 2005 *Plasma Phys. Control. Fusion* **47**, A317.

[8] Li, G. et al. 1995 *Phys. Plasmas* **2**, 2615.

[9] Brunsell, P. R. et al. 1994 *Phys. Plasmas* **1**, 2297.

[10] Rempel, T. D. et al. 1991 *Phys. Rev. Lett.* **67**, 1438.

[11] Lin, H. 1991 PhD thesis, Report FRCR no. 401, University of Texas, Fusion Research Center, Austin, TX, USA.

[12] Heller M. V. A. P., Castro, R. M., Brasílio, Z. A., Caldas, I. L. and Silva, R. P. 1995 *Nucl. Fusion* **35**, 59.

[13] Heller, M. V. A. P., Castro, R. M., Caldas, I. L., Brasílio, Z. A., Silva, R. P. and Nascimento, I. C. 1997 *J. Phys. Soc. Japan* **66**, 3453.

[14] Heller, M. V. A. P., Brasilio, Z. A., Caldas I. L. and Castro, R. M. 1999 *J. Phys. Soc. Japan* **68**, 1309.

[15] Devynck, P. et al. 2005 *Plasma Phys. Control. Fusion* **47**, 269.

[16] Jakubowski, M. W., Abdullaev, S. S., Finken, K. H. and the TEXTOR team. 2004 *Nucl. Fusion* **44**, 51.

[17] Ghendrih, Ph., Grosman, A. and Capes, H. 1996 *Plasma Phys. Control. Fusion* **38**, 1653.

[18] Shoji, T. et al. 1992 *J. Nucl. Mater.* **196–198**, 296.

[19] Takamura, S. 1989 *J. Nucl. Mater.* **162–164**, 643.

[20] Moyer, R. A. et al. 2005 *Phys. Plasmas* **12**, 056119 9.

[21] Karger, F. and Lackner, K. 1977 *Phys. Lett.* A **61**, 385.

[22] Caldas, I. L., Viana, R. L., Araujo, M. S. T., Vannucci, A., Silva, E. C., Ullmann, K. and Heller, M. V. A. P. 2002 *Brazil. J. Phys.* **32**, 980.

[23] McCool, S. C., Wootton, A. J., Aydemir, A. Y., Bengtson, R. D. and Oedo, J. A. 1989 *Nucl. Fusion* **29**, 547.

[24] Takamura, S., Ohinishi, N., Yamada, H. and Okuda, T. 1987 *Phys. Fluids* **30**, 144.

[25] Takamura, S., Yamada, H. and Okuda, T. 1988 *Nucl. Fusion* **28**, 183.

[26] Grosman, A. et al. 1992 *J. Nucl. Mater.* **196–198**, 59.
Evans, T. E. et al. 1992 *J. Nucl. Mater.* **196–198**, 421.

[27] Evans, T. E. et al. 1989 *Bull. Amer Phys. Soc.* **34**, 2168.

[28] Evans, T. E. et al. 1990 *Bull. Amer. Phys. Soc.* **35**, 1998.

[29] Budaev, V., Kikuchi, Y., Uesugi, Y. and Takamura, S. 2004 *Nucl. Fusion* **44**, S108.

[30] Pires, C. J. A., Saettone, E. A. O., Kucinski, M. Y., Vannucci, A. and Viana, R. L. 2005 *Plasma Phys. Control. Fusion* **47**, 1609.

[31] Heller, M. V. A. P., Caldas, I. L., Ferreira, A. A., Saettone, E. A. O., Vannucci, A., Nascimento, I. C. and Severo, J. H. F. 2005 *Czech. J. Phys.* **55**, 265.

[32] Nascimento, I. C. et al. 2005 *Nucl. Fusion* **45**, 796.

[33] Galvão, R. M. O. et al. 2001 *Plasma Phys. Control. Fusion* **43**, A 299.

[34] Ferreira, A. A., Heller, M. V. A. P. and Caldas, I. L. 2000 *Phys. Plasmas* **7**, 3567.

[35] Saettone, E. A. O. 2004 PhD thesis, Institute of Physics, University of São Paulo, Brazil.

[36] Ferreira, A. A., Heller, M. V. A. P., Caldas, I. L., Lerche, E. A., Ruchko, L. F. and Baccala, L. A. 2004 *Plasma Phys. Control. Fusion* **46**, 669.

[37] Van Milligen, B. Ph., Hidalgo, C., Sánchez, E., Pedrosa, M. A., Balbín, R., García-Cortes, I. and Tynan, G. R. 1997 *Rev. Sci. Instrum.* **68**, 967.

[38] Hidalgo, C., Pedrosa, M. A. and Gonçalves, B. 2002 *New J. Phys.* **4**, 511.

[39] Kausche, U., Schlueter, H. 1991 *Plasma Phys. Control. Fusion* **33**, 1309; 1992 *Plasma Phys. Control. Fusion* **34**, 935.

[40] Van Milligen, B. Ph., Sánchez, E., Estrada, T., Hidalgo, C., Brañas, B., Carreras, B. and Garcia, L. 1995 *Phys. Plasmas* **2**, 3017.

[41] Diamond, P. H. et al. 2000 *Phys. Rev. Lett.* **84**, 4842.

[42] Batista, A. M., Caldas, I. L., Viana, R. L., Lopes, S. R., Horton, W. and Morrison, P. J. Nonlinear three-mode interaction and drift-wave turbulence in a tokamak edge model, submitted *Phys. Plasmas*.

[43] Antar, G. Y., Devynck, P., Garbet, X. and Luckhardt, S. C. 2001 *Phys. Plasmas* **8**, 1612.

[44] Antoni, V. et al. 2001 *Phys. Plasmas* **8**, 5171.

[45] Antoni, V. et al. 2001 *Europhys. Lett.* **54**, 51.

[46] Vianello, N. et al. 2002 *Plasma Phys. Control. Fusion* **44**, 2513.

[47] Roberto, M., Silva, E. C., Caldas, I. L. and Viana, R. L. 2004 *Phys. Plasmas* **11**, 214.